

Practical Session

RANS simulation of a turbulent swirl-stabilized flame

MOD 4.3: Combustion for propulsion

Jérémy Archier

Nezha Bourakkadi



ÉCOLE
CENTRALE LYON

Practical Session

RANS simulation of a turbulent swirl-stabilized flame

by

Jérémy Archier
Nezha Bourakkadi

Student Name	Student Number
Jérémy Archier	1219441
Nezha Bourakkadi	11381

Instructor: Alexis. Giauque & Antoine Renaud
Teaching Assistant: Mikhael Gorokovski
Project Date: October, 2022
Faculty: Laboratoire de Mécanique des Fluides et d'Acoustique, ECL

Cover: Bâtiment de Tribologie, Mécanique et Matériaux (TMM1)
Style: EPFL Report Style, with modifications by Jérémy Archier

Contents

Nomenclature	iii
1 Introduction	1
2 Model description	2
2.1 Equations and definitions	2
2.1.1 Progress variable	2
2.1.2 Turbulent flame speed	2
2.1.3 RMS velocity	2
2.1.4 Swirl number	3
2.1.5 Stretch factor	3
2.1.6 Transport equation and temperature	3
2.2 Fluent model	4
3 Results and analysis	6
3.1 Initial modelling	6
3.1.1 Isocontours	6
3.1.2 Flow analysis	7
3.2 Effect of local flame extinction by stretching	8
3.2.1 Isocontours	8
3.2.2 Flow analysis	9
4 Conclusion and recommendations	10
References	11
A Additional figures	12
B Task Division	13

List of Figures

1.1	Illustration of a Safran Aircraft Engine [2]	1
2.1	Model initialization diagram	3
2.2	Analysis section profiles	4
2.3	Illustration of the mesh used in this model	5
3.1	Isocontours of the progress variable c in a longitudinal cut	6
3.2	Isocontours of the velocity magnitude in a longitudinal cut	7
3.3	Different velocity profiles for cross-sections	7
3.4	Isocontours of the progress variable c in a longitudinal cut	8
3.5	Isocontours of the velocity magnitude	8
3.6	Different velocity profiles for cross-sections	9
A.1	Progress variable c for different sections with no stretching	12
A.2	Progress variable c for different sections with stretching	12

Nomenclature

Abbreviations

Abbreviation	Definition
CFD	Computational Fluid Dynamics
RMS	Root-Mean-Square

Symbols

Symbol	Definition	Unit
v_x	Axial velocity at the inlet	$[m/s]$
v_θ	Azimuthal velocity at the inlet	$[m/s]$
v_l	Laminar flame velocity	$[m/s]$
T_{ad}	Adiabatic end of combustion temperature	$[K]$
c	Reaction progress variable	$[.]$
S	Swirl number	$[.]$
G	Stretch factor	$[.]$
U_{RMS}	Root-Mean-Square velocity	$[m/s]$
U_t	Turbulent flame speed	$[m/s]$
k	Turbulence kinetic energy of the flame	$[m^2/s^2]$
ρ	Density	$[kg/m^3]$

1

Introduction



Figure 1.1: Illustration of a Safran Aircraft Engine [2]

This first practical session was focused on the numerical study and CFD simulation of the injector of the combustion chamber of the next SNECFRAN engine. [1]

In order to do so, a numerical model of the combustion chamber and its associated mesh was given, as well as the desired model parameters (speeds, turbulence, temperature...etc).

The main goal of this simulation will be to identify stationary behaviors of the flame, depending on the topology, geometry and model parameters that are chosen. We will therefore be able to use the C-equation model for premixed combustion in order to analyze the topology of a premixed turbulent methane flame as a function of the inlet swirl number. We will then study the effect of stretch on the stability of the flame and consider possible improvements for this CFD model and simulation.

2

Model description

2.1. Equations and definitions

First of all, we will be introducing the parameters and equations used in this simulation based on a premixed turbulent combustion model where we assume that fuel and oxidizer are mixed prior to ignition. [3] In such systems, the combustion of unburnt reactants occurs as the flame front moves (the flow therefore moves at laminar flame speed v_l), converting unburnt reactants to burnt products. We can introduce several variables to characterize this combustion model:

2.1.1. Progress variable

The progress variable c is defined as follows:

$$c = \frac{\sum_{i=1}^n Y_i}{\sum_{i=1}^n Y_{i,ad}} \quad (2.1)$$

where n corresponds to the number of products, Y_i the mass fraction of species i and $Y_{i,ad}$ the mass fraction of species i after complete adiabatic combustion.

As a result, $c=0$ corresponds to the situation where the mixture is unburnt and $c=1$ where it is burnt. It is defined as a boundary condition: $c=0$ at the inlet and $c=1$ at the far end of the combustion chamber (outlet).

2.1.2. Turbulent flame speed

The turbulent flame speed U_t is normal to the surface of the flame and is influenced by the laminar flame speed v_l and the flame topology. Within the FLUENT software, it is computed using the following model:

$$U_t = AU_{RMS} \left(\frac{\tau_t}{\tau_c} \right)^{1/4} \quad (2.2)$$

where A corresponds to a model constant chosen here to be 0.52, U_{RMS} the root-mean-square velocity (m/s), τ_t is the turbulence time scale (s) and τ_c the chemical time scale (s)

2.1.3. RMS velocity

The RMS velocity U_{RMS} which characterizes turbulence (vortices) and in a way can be interpreted as the speed at which turbulence spreads in the flame front.

$$U_{RMS} = \sqrt{\frac{2k}{3}} \quad (2.3)$$

where k corresponds to the turbulence kinetic energy of the flame

2.1.4. Swirl number

Because we are studying a turbulent swirl-stabilized flame, we can also define its swirl number S in a homogeneous medium :

$$S = \frac{\int_{R_0}^{R_1} UV_{\theta} r dr}{\int_{R_0}^{R_1} U^2 r dr} \quad (2.4)$$

where U is the speed magnitude in m/s, V_{θ} is the tangential velocity and R_0 and R_1 correspond to dimensions of the combustion chamber in m

This swirling motion is used to help stabilize the flame by creating a low-pressure zone in the middle of the combustion chamber. The initial swirl number value used is **0.8**.

2.1.5. Stretch factor

We will also take into account the effects of flame stretch in the second part of this report. To model this behavior, the source term is multiplied by a stretch factor G which represents the probability that the stretching will not quench the flame. With no stretching, $G=1$.

$$G = \frac{1}{2} \operatorname{erfc} \left[-\sqrt{\frac{1}{2\sigma}} \left[\ln \left(\frac{\epsilon_{cr}}{\epsilon} \right) + \frac{\sigma}{2} \right] \right] \quad (2.5)$$

where erfc is the complementary error function, σ is the standard deviation of the distribution of ϵ and ϵ_{cr} is the turbulence dissipation rate at the critical rate of strain

2.1.6. Transport equation and temperature

To model the flame front propagation in this premixed combustion condition, FLUENT then solves the following transport equation for the progress variable c , where the source term ρS_c is computed using the various parameters detailed above.

$$\frac{\partial}{\partial t}(\rho c) + \nabla(\rho v c) = \nabla \left(\frac{\mu_t}{S_{c_t}} \nabla c \right) + \rho S_c \quad (2.6)$$

where c is the reaction progress variable, S_{c_t} is the turbulent Schmidt number for the gradient turbulent flux and S_c is the reaction progress source term in s^{-1}

In the case of an adiabatic premixed combustion model the temperature is calculated as follows:

$$T = (1 - c)T_u + cT_{ad} \quad (2.7)$$

where T_u is the temperature of the unburnt mixture and T_{ad} is the temperature of the burnt products under adiabatic conditions

The initial values of these different parameters are represented on the Figure below:

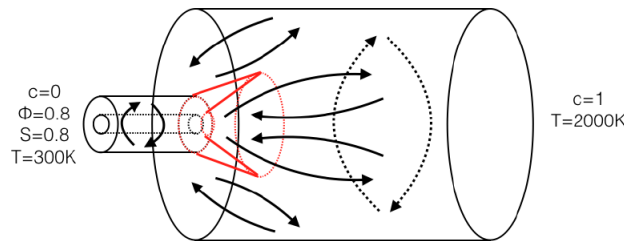


Figure 2.1: Model initialization diagram

In the scope of our analysis, we will be considering the evolution of axial speed U_x , radial speed U_r , tangential speed U_{θ} , RMS speed U_{RMS} and progress variable c (or temperature T) in the section profiles represented below:

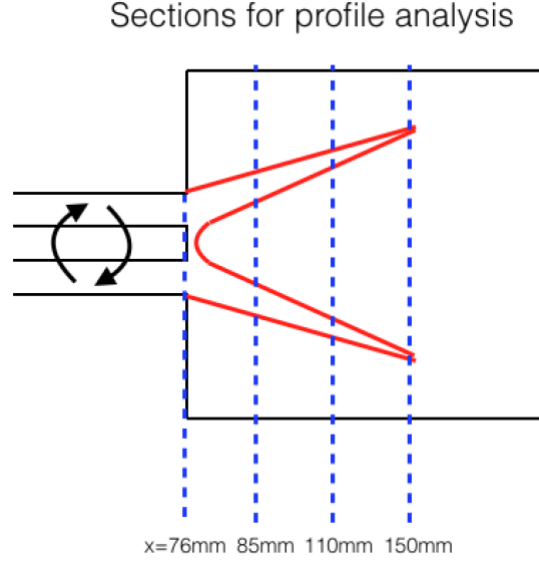


Figure 2.2: Analysis section profiles

2.2. Fluent model

As described in the previous section, we will be considering a premixed combustion model where fuel and oxidizer are mixed before entering the combustion chamber, prior to ignition. We will also assume an adiabatic combustion even though it is not the case in real configurations where walls are cooled with water to avoid them melting with extreme temperatures inside the combustion chamber. The methane flame is assumed to be a deflagration, meaning that the flow is subsonic and turbulent. Only inert particles are used in this model. The turbulence is represented by a k-epsilon model. The standard k-epsilon model is a semi-empirical model based on two transport equations for the turbulence kinetic energy (k) and its dissipation rate (ϵ). In this model, the flow is assumed to be fully turbulent and the effects of molecular viscosity are negligible. The transport equations are the following :

$$\frac{\partial}{\partial t}(\rho k) + \frac{\partial}{\partial x_i}(\rho k u_i) = \frac{\partial}{\partial x_j} \left[\left(\mu + \frac{\mu_t}{\sigma_k} \right) \frac{\partial k}{\partial x_j} \right] + G_k + G_b - \rho \epsilon - Y_M + S_k \quad (2.8)$$

$$\frac{\partial}{\partial t}(\rho \epsilon) + \frac{\partial}{\partial x_i}(\rho \epsilon u_i) = \frac{\partial}{\partial x_j} \left[\left(\mu + \frac{\mu_t}{\sigma_\epsilon} \right) \frac{\partial \epsilon}{\partial x_j} \right] + C_{1\epsilon} \frac{\epsilon}{k} (G_k + C_{3\epsilon} G_b) - C_{2\epsilon} \rho \frac{\epsilon^2}{k} + S_\epsilon \quad (2.9)$$

In these equations, G_k represents the generation of turbulence kinetic energy due to the mean velocity gradients, G_b is the generation of turbulence kinetic energy due to buoyancy, Y_M represents the contribution of the fluctuating dilatation in compressible turbulence to the overall dissipation rate. S_k and S_ϵ are user-defined source terms. The turbulence viscosity is computed from k and ϵ as follows:

$$\mu_t = \rho C_\mu \frac{k^2}{\epsilon} \quad (2.10)$$

The model constants have default values determined from experiments with air and water and are the standard ones and most widely used. The values are the following : $C_{1\epsilon}=1.44$ $C_{2\epsilon}=1.92$, $C_\mu=0.09$, $\sigma_k=1$ et $\sigma_\epsilon=1.3$.

A numerical model of the combustion chamber and its associated mesh was given and can be seen on the Figure below.

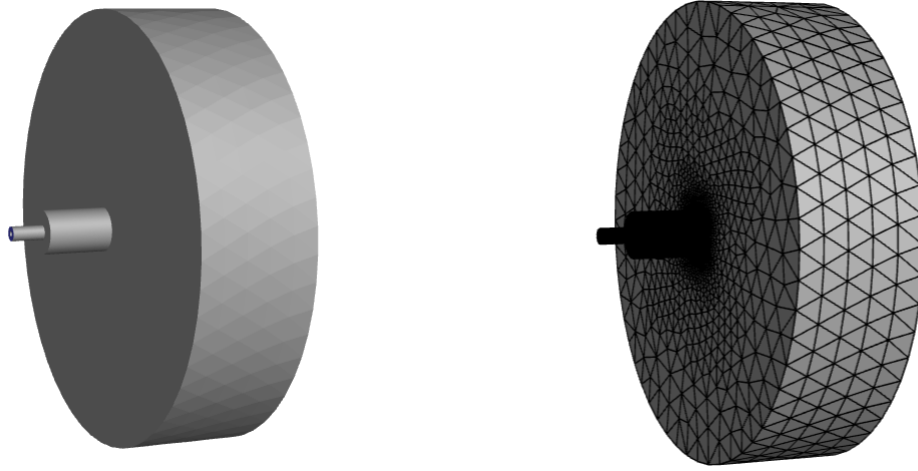


Figure 2.3: Illustration of the mesh used in this model

The mesh is a triangular mesh with the following characteristics.

Cells	Faces	Nodes	Boundary Nodes	Boundary Faces	Boundary Face Zones
384 697	782 553	72 189	13 161	26 318	5

Table 2.1: Mesh characteristics

We focused on a particular operating point which is the following.

- Inlet axial speed $v_x = 50 \text{ m.s}^{-1}$
- Inlet tangential speed $v_\theta = 40 \text{ m.s}^{-1}$
- Inlet turbulence intensity $I=5\%$
- Inlet turbulence length scale $l=0.01\text{m}$
- Adiabatic temperature at the end of combustion $T_{ad}=2000\text{K}$
- Laminar flame speed $v_l=0.25 \text{ m.s}^{-1}$

The default value of the stretch factor in FLUENT is 10^8 s^{-1} . When considering the flame stretch, we will be changing this value to identify the effects of such phenomena. The theoretical critical value for methane flames is $20\,000 \text{ s}^{-1}$.

This simulation took approximately 15 to 20 minutes to run, depending on the computer. In FLUENT, at the end of each solver iteration, the residual sum for each of the conserved variables is computed and stored to record the convergence history. As the solution converges, the residuals decrease to some small value and stop changing: the convergence criterion we used here was an absolute criterion of 10^{-5} which proved to be accurate enough in our modelling process.

Using the model previously described with the given parameter values, we will now be focusing on the results and analysing the topology of this methane flame as a function of the inlet swirl number and the effects of stretch on the stability of the flame.

3

Results and analysis

3.1. Initial modelling

We first run a simulation as explained in the previous chapter with a default stretch factor value of 10^8 s^{-1} with the given mesh in order to analyze the flame topology.

3.1.1. Isocontours

The model reduces the combustion chemistry down to a single reaction and characterizes the combustion process by a single progress variable c ($c = 0$ for the unburnt gas and $c = 1$ for the burnt products). The isocontours of this variable across a longitudinal cut are portrayed in the figure below.

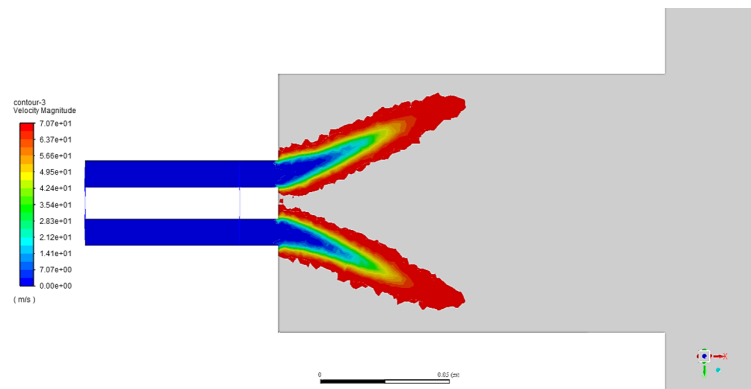


Figure 3.1: Isocontours of the progress variable c in a longitudinal cut

It can be noted that as the flame expands, the c variable increases. As it reaches 1 (i.e. all products are burnt), the flame will stop expanding. In the case of premixed combustion, the flame can be seen as an interface separating two regions - fresh and burnt gases.

The flame is also not strictly symmetrical, this may be due to the initial mesh which is quite coarse in some regions and therefore cannot accurately represent the flame topology in those regions. The mesh is less accurate in some areas of the model mainly for practical reasons: thanks to this simplification, the calculation time of the CFD simulation only takes about ten minutes to converge to the desired accuracy, where it would be much longer with a more detailed mesh while also providing us with more accurate results. As we are not aiming for accuracy but much more aiming at representing the global topology of the flame, this modelling choice proved quite relevant.

Furthermore, we can see that the flame has a V-shape and is - on average - not staying in the middle of the combustion chamber. Plotting the velocity magnitude will help us understand why the flame does not set in the chamber's centre.

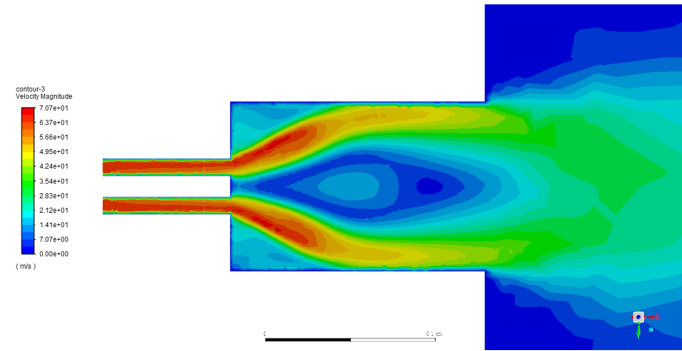


Figure 3.2: Isocontours of the velocity magnitude in a longitudinal cut

What is clear is that the flame is the driving force behind the flow, which is characteristic of a pre-mixed combustion model. Inside the flame, we can identify a low pressure zone where the fluid velocity is either non-existent or very low. There is in fact a backflow at the centre of the combustion chamber that helps in the flame stability, as illustrated in figure 2.1.

Moreover, we can notice that the fluid rotates along the cylinder walls, de facto maintaining the flow within a fictitious cylinder as it leaves the combustion chamber. This motion is essential to stabilize the flame with a backflow spreading strictly at the flame speed.

3.1.2. Flow analysis

A more detailed look at the flow through transverse and axial velocity profiles, temperature, momentum and turbulent kinetic energy is now provided in the numerous charts hereafter in figure 3.3.

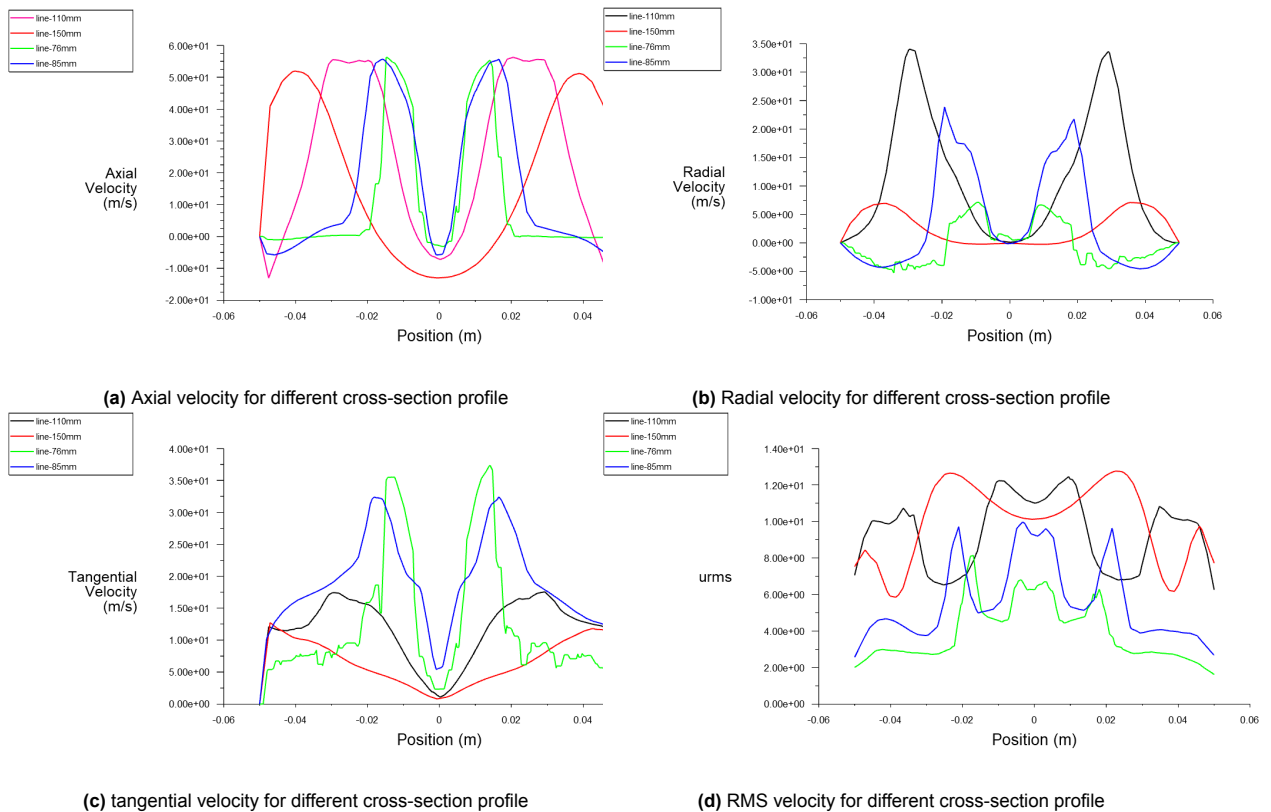


Figure 3.3: Different velocity profiles for cross-sections

All velocity profiles have the same shape: this is due to the fact that they are derived from the progress variable c which is computed through the c -equation (see Figure A.1). The velocities are therefore higher in the zones where the fuel has been burnt, which supports the idea that combustion indeed drives the flow.

However, the turbulence intensity characterized by U_{RMS} does not seem to abide by this law. Indeed, turbulence appears to be building up as it gets further from the injector and is generally larger in the centre of the combustion chamber.

3.2. Effect of local flame extinction by stretching

A sensitivity analysis on the stretch factor was performed to analyse the effect of local flame extinction by stretching.

We observed that a stationary solution cannot be found in all cases. If the stretching factor is reduced to less than 10^{-4} the solver is no longer converging (the theoretical value is $2.0 \cdot 10^4 s^{-1}$).

3.2.1. Isocontours

In this section, the value of the stretching factor is set at $2.0 \cdot 10^4$ to improve the model and have a flame model that is closer to real conditions. The isocontours of the progress variable in a cross-section are portrayed in the Figure below.

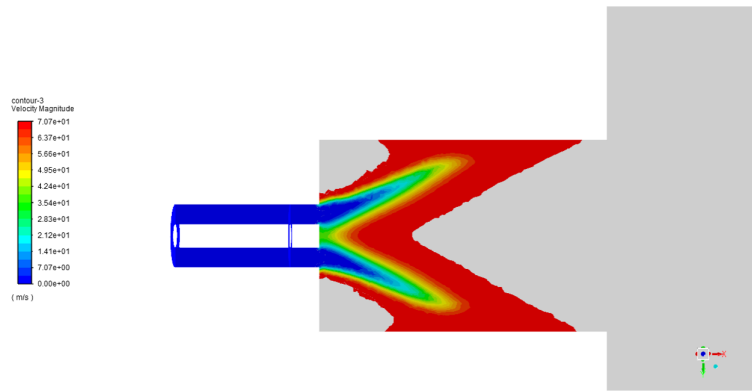


Figure 3.4: Isocontours of the progress variable c in a longitudinal cut

We can indeed note that this flame is more stretched than the previous one : this representation is therefore more realistic because with no stretching involved, the other flame would never extinguished by any blow to it. Besides, the V-shape of the flame is preserved, though being more spread out.

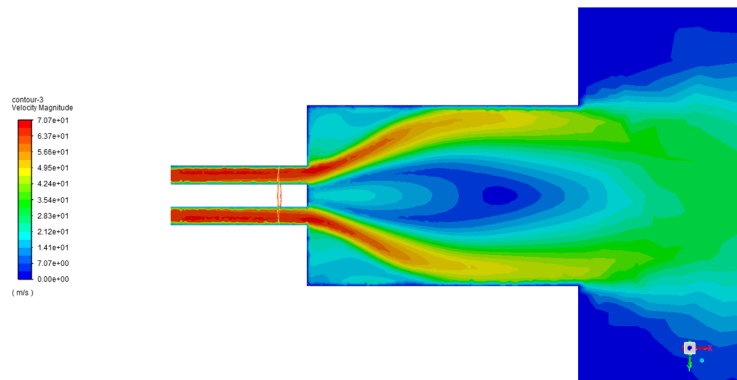


Figure 3.5: Isocontours of the velocity magnitude

The velocity magnitude is represented on the figure above. We can see very few differences from the configuration where stretching was not taken into account. As for the flame topology, the low pressure zone with almost zero fluid velocity at the centre of the combustion chamber is even larger than before, as illustrated in figure 3.5. That also means that there is significantly larger recirculation at the centre of the chamber: a bigger backflow is indeed necessary to keep the flame stable since stretching induces more unstability.

3.2.2. Flow analysis

Once again, we are considering the flow through transverse and axial velocity profiles to analyse the impact of the stretching factor on the fluid flow in the figure hereinbelow.

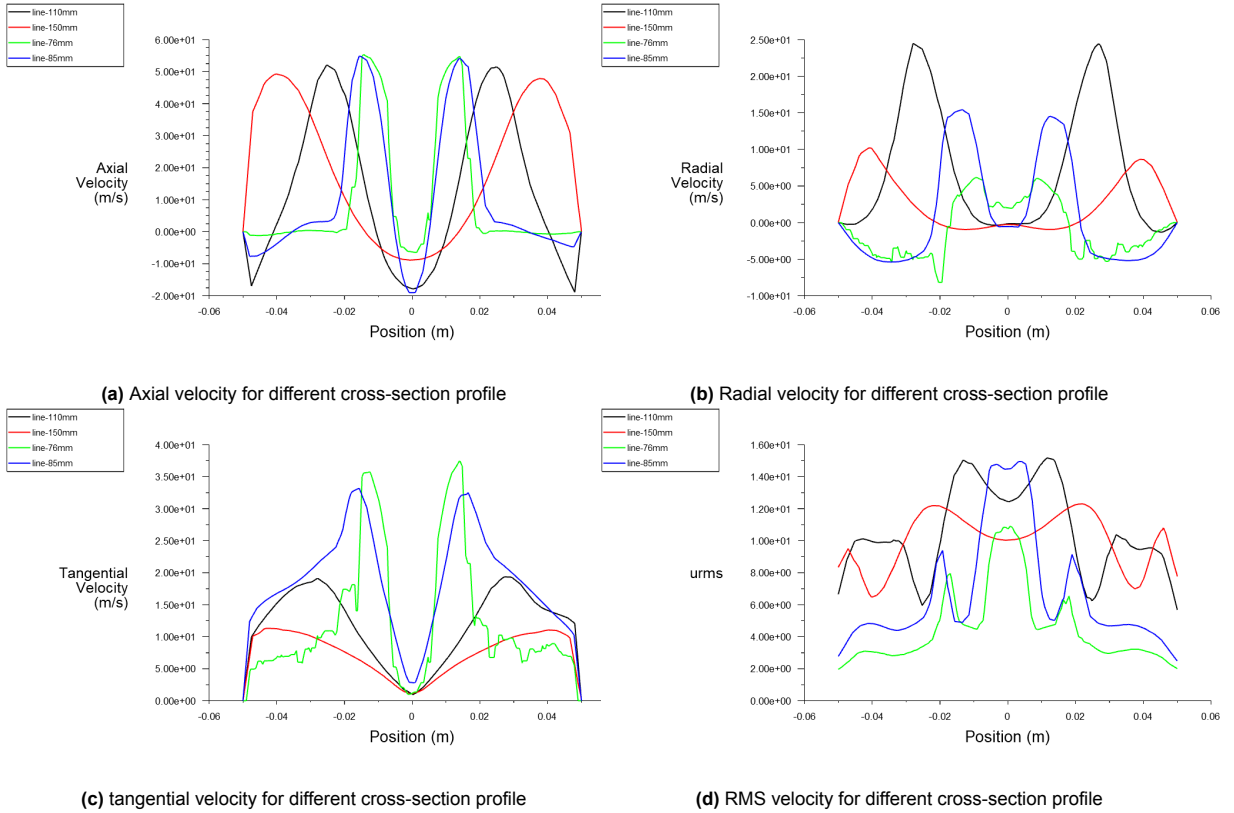


Figure 3.6: Different velocity profiles for cross-sections

The first thing to note is that the velocity values are mostly lower than they were in the model with no stretching. However, turbulence intensity (U_{RMS}) is higher with the realistic stretching model and is highly concentrated in the centre of the combustion chamber. This can again be attributed to the stretching phenomenon which introduces more unstability and consequently more turbulence in the system, especially at the centre of the combustion chamber where a backflow sets.

Regarding the progress variable (see figure A.2), we could notice that the flame thickness increased when setting the stretching factor to a realistic value.

4

Conclusion and recommendations

To conclude, thanks to this practical session, we were able to analyse the topology of a premixed turbulent methane flame thanks to a C-equation model for premixed combustion on the FLUENT software. To this end, we used a simplified approach that allowed us to get a glimpse at the phenomenon taking place in the combustion chamber and understand the reactions and behaviours at stake. While we were not aiming for accuracy but mainly at a global representation, the simplifications that were made introduced several inaccuracies when comparing our results with real-life conditions. First, in real systems, the flame can be observed sitting right on top of the injector- with a region separating it from the injector. But because we assumed an adiabatic model (ie. with no heat transfers), this could not be observed in our model. Heat exchanges are indeed not taken into account here but in reality, the walls are cooled with water to avoid them melting because of the extreme temperatures. As a result, the temperature inside the combustion chamber and the temperature of its walls are different. This temperature difference is not accurately represented in this adiabatic model which therefore cannot properly represent the real behaviour of the flame.

To improve this model, we should thus change the wall conditions to allow heat transfers to occur between the fluid and the exterior by setting a wall temperature for example. Changing the turbulence model could prove to be an interesting thing to do as well, to study the influence of turbulence on flame stability. As mentioned above, we could also change the mesh and its properties to get a more accurate representation of the flame topology in all regions of the combustion chamber, taking into account different parameters (swirl number, stretching factor, turbulence...etc) as done during this practical session to understand their influence on the real flame topology and behaviour.

References

- [1] A. Giauque and M. Gorokovski. *Numerical Analysis of turbulent swirl-stabilized flame*. Practical session 1 - Ecole Centrale de Lyon. 2022.
- [2] Safran Group. *Safran Aircraft Engines*. 2022. URL: <https://www.safran-group.com/fr/societes/safran-aircraft-engines> (visited on 10/14/2022).
- [3] ANSYS Inc. *ANSYS FLUENT 12.0 User's Guide*. 12.0. Jan. 2009.

A

Additional figures

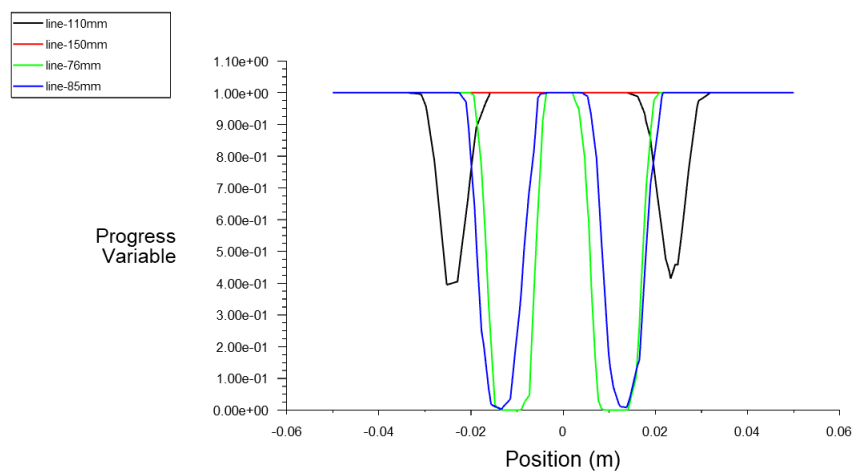


Figure A.1: Progress variable c for different sections with no stretching

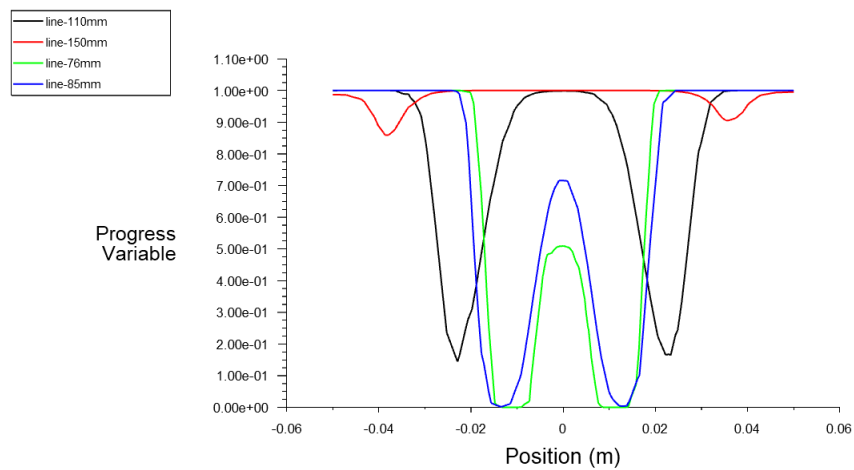


Figure A.2: Progress variable c for different sections with stretching

B

Task Division

Table B.1: Distribution of the workload

	Task	Student Name(s)
Chapter 1	Introduction	Nezha Bourakkadi
Chapter 2	Model description	Nezha Bourakkadi
Chapter 3	Results and analysis	Jérémy Archier
Chapter 4	Conclusion	Jérémy Archier & Nezha Bourakkadi
	Editors	Jérémy Archier & Nezha Bourakkadi
	CAD and Figures	Jérémy Archier & Nezha Bourakkadi
	Document Design and Layout	Jérémy Archier